Hindawi
Computational and Mathematical Methods
Volume 2022, Article ID 9667396, 18 pages
https://doi.org/10.1155/2022/9667396

Research Article

Modeling and Optimal Control Analysis for Malaria Transmission with Role of Climate Variability

Temesgen Duressa Keno,[1] **Lemessa Bedjisa Dano**,[1] **and Oluwole Daniel Makinde**[2]

[1]*Department of Mathematics, Wallaga University, Nekemte, Ethiopia*
[2]*Faculty of Military Science, Stellenbosch University, Stellenbosch, South Africa*

Correspondence should be addressed to Temesgen Duressa Keno; temesgenduressaa@gmail.com

Received 19 September 2022; Revised 28 October 2022; Accepted 14 November 2022; Published 2 December 2022

Academic Editor: Suresh Rasappan

In this paper, we present a nonlinear deterministic mathematical model for malaria transmission dynamics incorporating climatic variability as a factor. First, we showed the limited region and nonnegativity of the solution, which demonstrate that the model is biologically relevant and mathematically well-posed. Furthermore, the fundamental reproduction number was determined using the next-generation matrix approach, and the sensitivity of model parameters was investigated to determine the most affecting parameter. The Jacobian matrix and the Lyapunov function are used to illustrate the local and global stability of the equilibrium locations. If the fundamental reproduction number is smaller than one, a disease-free equilibrium point is both locally and globally asymptotically stable, but endemic equilibrium occurs otherwise. The model exhibits forward and backward bifurcation. Moreover, we applied the optimal control theory to describe the optimal control model that incorporates three controls, namely, using treated bed net, treatment of infected with antimalaria drugs, and indoor residual spraying strategy. The Pontryagin's maximum principle is introduced to obtain the necessary condition for the optimal control problem. Finally, the numerical simulation of optimality system and cost-effectiveness analysis reveals that the combination of treated bed net and treatment is the most optimal and least-cost strategy to minimize the malaria.

1. Introduction

Malaria is a vector-borne disease caused by a parasite called *Plasmodium* and transmitted between humans and mosquitos via bites of infected female *Anopheles* mosquitoes. It is a major public health problem, particularly on the African continent [1]. This disease can also be transmitted by blood transfusion or congenital. According to the world malaria report published in December 2021, an estimated 241 million cases and 627000 deaths occurred worldwide, with the African Region accounting for 95 percent of all cases in 2020 [2]. Climate variability is recognized to have a significant impact on the malaria vector's life cycle, and the life of the mosquito is governed by temperature and rainfall [3]. The most effective way to avoid the malaria dynamics are treated bed net, treatment with antimalaria drugs, and indoor residual spraying [4].

The mathematical model for malaria dynamics is the most useful in comprehending the disease's presence in the human population. Ross devised the first mathematical model for malaria dynamics transmission [5]. Various mathematical models based on Ross's basic malaria model were described by different scholars with different factors such as including the exposed class in mosquitoes and humans [6–8] and the impact of climate variations on malaria epidemics in terms of death rate, birth rate, and prevalence of mosquito population [9–11].

Many investigations of malaria dynamics models were presented using optimum control problems employing optimal control theory. For example, Agusto et al. [12] investigated optimum solutions for decreasing the dynamics of malaria using a malaria transmission model with an optimal control problem. The authors proposed that the combination of the treated bed net, therapy, and indoor residual spraying is

Table 1: Parameters description used for the model (1).

Parameters	Parameter description
μ_h	Human death rate due to natural cause
δ	Induced death rate of human
γ_h	Recover rate of infected humans
Ψ	Human recruitment rate
Φ_0	Mosquito recruitment rate
μ_m	Mosquito natural death rate
ω_h	Human immune deficiency rate
β_{1m}	Mosquito contact rate (incremental)
β_{1h}	Human contact rate (incremental)
Φ_{1m}	Incremental birth rate of mosquito
β_{0h}	Contact rate of human with mosquito
β_{0m}	Contact rate of mosquito with human
α_h	Exposed human progression rate
α_m	Exposed mosquito progression rate
m	Temperature dependent rate of precipitation
z^*	Percentage of an antibody produced by a human
m^*	Percentage of an antibody produced by a mosquito
r	Temperature increase rate
T_0	Minimum temperature for the mosquito to be less active
$T_{\max}$	Maximum temperature for the mosquito to be most active

the optimum technique for illness reduction. Okosun et al. [13] created a malaria model that includes optimum control techniques of malaria disease transmission with two measures that regulate treatment infectious and immunization. The authors determined that the combination of therapy and immunization is the most effective and least expensive way to control a malaria condition. Leiton et al. [14] presented an SEIRS-SI optimal control model for malaria transmission in Colombia considering three optimal control strategies. The authors concluded that integrated of control measures treated bed net, intermittent prophylactic treatment in pregnancy and effective case management is the best strategy to prevent the malaria dynamics. Olaniyi et al. [15] formulated a malaria transmission dynamic model with an optimal control analysis using four time dependent continuous controls. The authors concluded that the combination of all these controls is the best measure to minimize the spread of malaria. Keno et al. [16] formulated an optimal control and cost effectiveness strategies of malaria transmission with temperature variability factor by considering three optimal control strategies. The model analysis provides that the combination of treatment and indoor residual spraying is the most efficient and less costly strategy to minimize the malaria. Olaniyi et al. [17] proposed SEIRS for the human population and SEI malaria model with optimal control and cost-effectiveness analysis in the presence of reinfection and relapse in malaria dynamics. The authors suggested that the strategy with a combination of treated bed net and indoor residual spraying is the most effective and least cost to eradicate the malaria.

To the best of our knowledge, the impact of climate variability on malaria epidemics with optimal control and cost effectiveness analysis with a logistic growth of climate variation with respect to mosquitoes breeding and malaria infection was not considered in their models. In the malaria transmission model [11], we considered impact of temperature variability on malaria epidemics. In this paper, we extended model [11] to the impact of climate variability (temperature and rainfall) with respect to mosquitoes breeding rate and malaria infection with optimal control and cost effectiveness analysis.

The following is the format of this paper: in Section 2, we develop a malaria transmission model that incorporates the impact of climate variability on malaria epidemics. The model's qualitative analysis is described in Section 3. We perform sensitivity analysis in Section 4. The optimal control analysis of the malaria transmission model is described in Section 5. In Section 6, we compared numerical simulation results to analytical results. The cost-effectiveness analysis is depicted in Section 7. Finally, Section 8 discusses the study's conclusion.

2. Model Description and Formulation

In this section, we proposed and developed a malaria transmission model that takes into account the human and vector populations, with the total human population denoted by $N_h(t)$ and the vector population denoted by $N_m(t)$. The SEIRS model describes the human population and divides it at time t into the following subpopulations: susceptible human $S_h(t)$,

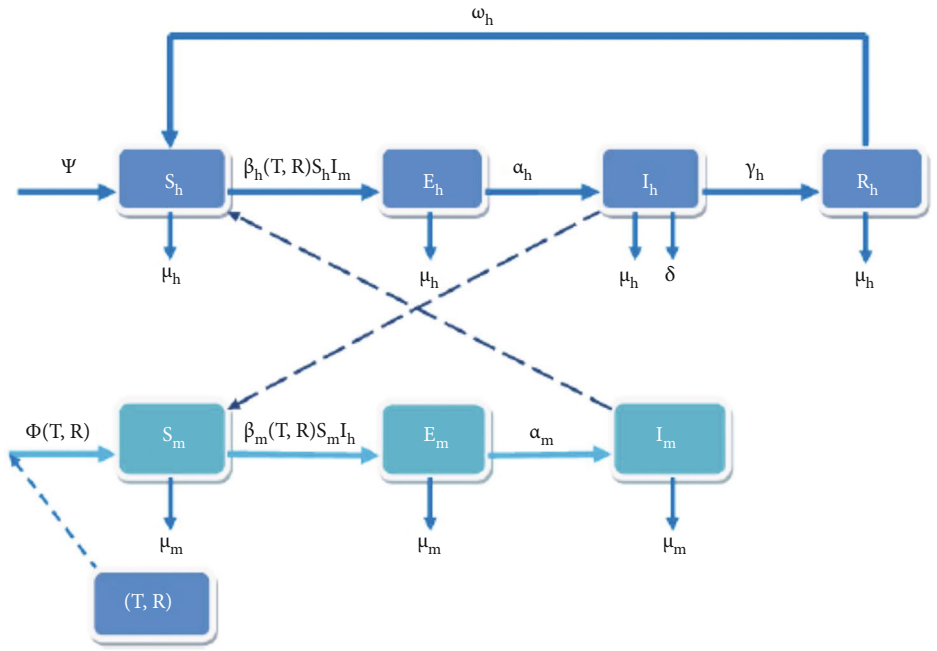

Figure 1: Flow diagram of malaria transmission.

exposed human $E_h(t)$, infected human $I_h(t)$, and recovered human $R_h(t)$. The SEI model describes the mosquito population, and the total mosquito population at time t, denoted by $N_m(t)$, is subdivided into susceptible mosquito $S_m(t)$, exposed mosquito $E_m(t)$, and infected mosquito $I_m(t)$. The total human and mosquito populations are then given by $N_h(t) = S_h(t) + E_h(t) + I_h(t) + R_h(t)$ and $N_m(t) = S_m(t) + E_m(t) + I_m(t)$, respectively. Assume that all of the parameters in the model are positive. The new recruits (assumed to be susceptible) enter the human population by birth (migration) at the rate Ψ. An infectious mosquito transmits malaria to the susceptible human, and the susceptible human moves to the exposed human at a climate dependent rate of $\beta_h(T, R)$, β_{0h} is the contact rate of humans with mosquitos when there is no variation in climate, and β_{1h} is the incremental contact rate of humans with mosquitos due to climate variation. The progression of exposed humans to infected humans is α_h, the natural death rate of all humans is μ_h, and induced death is δ. The infected human recovered due to the use of antimalarial drugs through a treatment rate of γ_h. The recovered populations of humans have short period immunity that can be lost and become susceptible to reinfection rate of ω_h. The recruitment of mosquito populations at a rate of $\Phi(T, R)$ is climate-dependent; Φ_0 is the birth rate of mosquitos when there is no variation in climate, and ϕ_{1m} is the incremental birth rate of mosquitos when there is variation in climate. Mosquito population contact with an infected human with malaria and moved to exposed class at a climate dependent rate of $\beta_m(T, R)$, β_{0m} is mosquito contact rate with human when there is no variation in climate, and β_{1m} is incremental mosquito contact rate with a human due to climate variation. The exposed mosquito moved at a rate of α_m to an infected mosquito. Every mosquito dies at the same rate μ_m. Mosquitoes do not recover from malaria because an infected mosquito is infectious until it dies. The temperature growth rate r follows a logistic function, m is the temperature dependent rate of precipitation, $T_{\max}$ is the maximum temperature for the mosquito to be most active, and T_0 is the minimum temperature for the mosquito to be less active. All the description of parameters are given in Table 1, and the diagram of malaria disease transmission is shown in Figure 1.

The transmission dynamics of malaria is described by the following system of nonlinear differential equations, based on the flow diagram depicted in Figure 1:

$$\begin{cases} \dfrac{dS_h}{dt} = \Psi - \dfrac{\beta_h(T,R)S_hI_m}{1+z^*I_m} - \mu_hS_h + \omega_hR_h, \\ \dfrac{dE_h}{dt} = \dfrac{\beta_h(T,R)S_hI_m}{1+z^*I_m} - (\mu_h+\alpha_h)E_h, \\ \dfrac{dI_h}{dt} = \alpha_hE_h - (\mu_h+\delta+\gamma_h)I_h, \\ \dfrac{dR_h}{dt} = \gamma_hI_h - (\mu_h+\omega_h)R_h, \\ \dfrac{dS_m}{dt} = \Phi(T,R) - \dfrac{\beta_m(T,R)S_mI_h}{1+\mathrm{m}^*\mathrm{I_h}} - \mu_mS_m, \\ \dfrac{dE_m}{dt} = \dfrac{\beta_m(T,R)S_mI_h}{1+\mathrm{m}^*\mathrm{I_h}} - (\mu_m+\alpha_m)E_m, \\ \dfrac{dI_m}{dt} = \alpha_mE_m - \mu_mI_m, \\ \dfrac{dT}{dt} = r\left(1-\dfrac{T}{T_{\max}}\right)(T-T_0), \\ \dfrac{dR}{dt} = \mathrm{m}\dfrac{dT}{dt} \Rightarrow R(t) = \mathrm{m}(T(t)-T_0) + \varepsilon, \end{cases} \tag{1}$$

where $\beta_h(T,R) = \beta_{0h} + \beta_{1h}k, \beta_m(T,R) = \beta_{0m} + \beta_{1m}k, \Phi(T,R) = \Phi_0 + \Phi_{1m}k$ and $k = ((1+m)(T-T_0)/T_{\max})$.

$$\begin{aligned}\text{With initial conditions } S_h(0) &= S_{h0}, E_h(0) = E_{h0}, I_h(0)\\ &= I_{h0}, R_h(0) = R_{h0}, S_m(0)\\ &= S_{m0}, E_m(0) = E_{m0}, I_m(0)\\ &= I_{m0}, T(0) = T_{\mathrm{m0}}, R(0) = R_{\mathrm{m0}}.\end{aligned} \tag{2}$$

Base on the fact that as average temperatures at the earth's surface rise more, evaporation occurs, which in turn increases overall precipitation (rainfall). Therefore, a warming climate is expected to increase precipitation (rainfall) in many areas. This implies that rainfall pattern is an increasing function of temperature. Note that m is the temperature dependent rate of precipitation, and ε is the amount of precipitation at $T = T_0$. In essence,

$$R_0 = \varepsilon \text{ at } T = T_0 \text{ and } R_{\max} = m(T_{\max} - T_0) + R_0. \tag{3}$$

3. Qualitative Analysis of the Model

3.1. Invariant Region. The invariant region is used to determine where the model's solution is bounded. The model (1) is divided into two parts: the host population and the vector population. The total human population is represented by $N_h(t) = S_h(t) + E_h(t) + I_h(t) + R_h(t)$. Then, by differentiating $N_h(t)$ both sides with respect to time and combining the first four equations from the model (1), we get

$$\frac{d}{dt}(S_h + E_h + I_h + R_h) = \Psi - \mu_h N_h - \delta I_h. \tag{4}$$

Then, equation (4) becomes

$$\frac{d}{dt}(S_h + E_h + I_h + R_h) \le \Psi - \mu_h N_h. \tag{5}$$

By solving the equation (5), we can see that $0 \le N_h \le \Psi/\mu_h$. Thus, for the human population, the bounded region of the system (1) is given by

$$\Omega_h = \left\{(S_h, E_h, I_h, R_h) \in \mathbb{R}_+^4 : 0 \le S_h + E_h + I_h + R_h \le \frac{\Psi}{\mu_h}\right\}. \tag{6}$$

Similarly, the equation gives the total mosquito population in the system (1) is

$$N_m(t) = S_m(t) + E_m(t) + I_m(t). \tag{7}$$

Obviously, the result we obtain after differentiating $N_m(t)$ with respect to time (t) is

$$\frac{d}{dt}(S_m + E_m + I_m) = \Phi(T,R) - \mu_m N_m. \tag{8}$$

By solving the equation (8), we get $0 < N_m \le \Phi(T,R)/\mu_m$. As just a result, for the mosquito population, the invariant region of the system (1) is given by

$$\Omega_m = \left\{(S_m, E_m, I_m) \in \mathbb{R}_+^3 : 0 \le S_m + E_m + I_m \le \frac{\Phi(T,R)}{\mu_m}\right\}, \tag{9}$$

is a positive invariant. As a result, the system's invariant region (1) is given by

$$\Omega = \Omega_h \times \Omega_m = \left\{(S_h, E_h, I_h, R_h, S_m, E_m, I_m) \in \mathbb{R}_+^7 : N_h \le \frac{\Psi}{\mu_h}, N_m \le \frac{\Phi(T,R)}{\mu_m}\right\}, \tag{10}$$

is a positive invariant set, and all of the solution set of system (1) is bounded in Ω within the region.

3.2. Positivity of the Solution. The purpose of this subsection is to demonstrate that all solutions of the model (1) will remain nonnegative in the future if their initial data is nonnegative.

Theorem 1. *The model solution (1) given by $S_h(t), E_h(t), I_h(t), R_h(t), S_m(t), E_m(t)$ and $I_m(t)$ with nonnegative initial conditions $S_h(0), E_h(0), I_h(0), R_h(0), S_m(0), E_m(0)$ and $I_m(0)$ remain nonnegative for all time $t \ge 0$.*

Proof. First, take the begin equation from system (1) as given by

$$\frac{dS_h}{dt} = \Psi - \frac{\beta_h(T,R)S_h I_m}{1 + z^* I_m} - \mu_h S_h + \omega_h R_h. \tag{11}$$

Consequently, this indicates that

$$\frac{dS_h}{dt} \ge -\left(\frac{\beta_h(T,R)I_m}{1 + z^* I_m} + \mu_h\right) S_h. \tag{12}$$

We obtain by integrating equation (12) with respect to time and solving it using the technique of variable separation with initial condition.

$$S_h(t) \ge S_h(0)\ \exp\left\{-\left(\mu_h t + \int_0^t \left(\frac{\beta_h(T,R)I_m(x)}{1 + z^* I_m(x)}\right)\right) dx\right\} \ge 0. \tag{13}$$

The other state variables $E_h(t), I_h(t), R_h(t), S_m(t), E_m(t)$, and $I_m(t)$ are nonnegative for all time $t \ge 0$ by the same procedure. As a result, the malaria transmission model

stated in system (1) is both epidemiologically significant and mathematically well posed in Ω. □

3.3. Basic Reproduction Number ($\mathfrak{R}_0$). To find the steady-state solution of the model (1), we equated the left-hand side of the system (1) to zero with the value of $E_h = 0, I_h = 0, E_m = 0, I_m = 0$, and obtained the disease free-equilibrium of system (1) denoted by E_1 or E_2, where

$$E_1 = \left(\frac{\Psi}{\mu_h}, 0, 0, 0, \frac{\Phi(T_0)}{\mu_m}, 0, 0, T_0, R_0\right) \text{or } E_2 = \left(\frac{\Psi}{\mu_h}, 0, 0, 0, \frac{\Phi(T_{\max})}{\mu_m}, 0, 0, T_{\max}, R_{\max}\right). \tag{14}$$

The basic reproduction number is defined as the average amount of secondary infectious caused by a primary infectious over a given time period [18], and it has been calculated using the next-generation matrix method [19]. Then, to get $\mathfrak{R}_{01}$ and $\mathfrak{R}_{02,}$ at E_1 and E_2, respectively, we rewrite the model (1) beginning with newly infective classes of human and mosquito population as

$$\begin{cases} \dfrac{dE_h}{dt} = \dfrac{\beta_h(T,R)S_hI_m}{1+z^*I_m} - (\mu_h+\alpha_h)E_h, \\ \dfrac{dI_h}{dt} = \alpha_hE_h - (\mu_h+\delta+\gamma_h)I_h, \\ \dfrac{dE_m}{dt} = \dfrac{\beta_m(T,R)S_mI_h}{1+m^*I_h} - (\mu_m+\alpha_m)E_m, \\ \dfrac{dI_m}{dt} = \alpha_mE_m - \mu_mI_m. \end{cases} \tag{15}$$

The right hand side of system (15) can then be written as $f - v$, where

$$f = \begin{pmatrix} \dfrac{\beta_h(T,R)S_hI_m}{1+m^*I_m} \\ 0 \\ \dfrac{\beta_m(T,R)S_mI_h}{1+m^*I_h} \\ 0 \end{pmatrix} \text{ and } v = \begin{pmatrix} (\mu_h+\alpha_h)E_h \\ (\mu_h+\delta+\gamma_h)I_h - \alpha_hE_h \\ (\mu_m+\alpha_m)E_m \\ \mu_mI_m - \alpha_mE_m \end{pmatrix}. \tag{16}$$

The Jacobian matrices of f and v at the disease-free equilibrium points give F and V, respectively, where

$$F = \begin{pmatrix} 0 & 0 & 0 & \beta_h(T^*,R^*)\dfrac{\Psi}{\mu_h} \\ 0 & 0 & 0 & 0 \\ 0 & \beta_m(T^*,R^*)\dfrac{\Phi(T^*,R^*)}{\mu_m} & 0 & 0 \\ 0 & 0 & 0 & 0 \end{pmatrix} \text{ and } V = \begin{pmatrix} \alpha_h+\mu_h & 0 & 0 & 0 \\ -\alpha_h & \mu_h+\delta+\gamma_h & 0 & 0 \\ 0 & 0 & \alpha_m+\mu_m & 0 \\ 0 & 0 & -\alpha_m & \mu_m \end{pmatrix}. \tag{17}$$

The next-generation matrix from the product of equation (17) calculated by FV^{-1} is obtained as

$$\mathrm{FV}^{-1} = \begin{pmatrix} 0 & 0 & \dfrac{\beta_h(T^*,R^*)\Psi\alpha_m}{\mu_h\mu_m(\alpha_m+\mu_m)} & \dfrac{\beta_h(T^*,R^*)\Psi}{\mu_h\mu_m} \\ 0 & 0 & 0 & 0 \\ \dfrac{\beta_m(T^*,R^*)\Phi(T^*,R^*)\alpha_h}{\mu_m(\alpha_h+\mu_h)(\alpha_h+\gamma_h+\mu_h)} & \dfrac{\beta_m(T^*,R^*)\Phi(T^*,R^*)}{\mu_m(\mu_h+\delta+\gamma_h)} & 0 & 0 \\ 0 & 0 & 0 & 0 \end{pmatrix}. \tag{18}$$

Thus, the fundamental reproduction number $\mathfrak{R}_0 = \rho(FV^{-1})$ where ρ is the dominant eigenvalue of the product FV^{-1} and the $\mathfrak{R}_{01}$ and $\mathfrak{R}_{02}$ at disease free equilibrium E_1 and E_2 are obtained, respectively, in equations (19) and (20) as given by

$$\mathfrak{R}_{01} = \sqrt{\frac{\beta_{0h}\Psi\beta_{0m}\Phi_0\alpha_h\alpha_m}{\mu_h\mu_m^2(\mu_h+\delta+\gamma_h)(\alpha_h+\mu_h)(\alpha_m+\mu_m)}}, \tag{19}$$

$$\mathfrak{R}_{02} = \sqrt{\frac{(\beta_{0h}+\beta_{2h})\Psi(\beta_{0m}+\beta_{2m})(\Phi_0+\Phi_{2m})\alpha_h\alpha_m}{\mu_h\mu_m^2(\mu_h+\delta+\gamma_h)(\alpha_h+\mu_h)(\alpha_m+\mu_m)}}, \tag{20}$$

where $\beta_{2h} = \beta_{1h}k, \beta_{2m} = \beta_{1m}k, \Phi_{2m} = \Phi_{1m}k$, and $k = ((1+m)(T_{\max} - T_0)/T_{\max})$.

As a result, the basic reproduction number ($\mathfrak{R}_{02}$) at maximum temperature can be written in terms of $\mathfrak{R}_{01}$ in the equation (21), as described below:

$$\mathfrak{R}_{02} = \sqrt{\mathfrak{R}_{01}^2 + \frac{\Phi_0\beta_{0m}\beta_{2m}\Psi\alpha_h\alpha_m + \Psi(\beta_{0m}+\beta_{2m})[\beta_{2h}(\Phi_0+\Phi_{2m})+\Phi_{2m}\beta_{0h}]\alpha_h\alpha_m}{\mu_h\mu_m^2(\mu_h+\delta+\gamma_h)(\alpha_h+\mu_h)(\alpha_m+\mu_m)}}, \tag{21}$$

where $\mathfrak{R}_{01}$ denotes the basic reproduction number at T_0 for the mosquito to be less active in breeding.

3.4. Local Stability of Disease-Free Equilibrium

Theorem 2. *If $\mathfrak{R}_{01} < \mathfrak{R}_{02} < 1$; then, the disease free equilibrium point(s) of the system (1) is locally asymptotically stable in Ω.*

Proof. The Jacobian matrix of equation (1) at the disease-free equilibrium point is given as

$$z(E_*) = \begin{pmatrix} z_{11} & 0 & 0 & \omega_h & 0 & 0 & -\beta_h(T^*,R^*)\frac{\Psi}{\mu_h} \\ 0 & z_{22} & 0 & 0 & 0 & 0 & \beta_h(T^*,R^*)\frac{\Psi}{\mu_h} \\ 0 & \alpha_h & z_{33} & 0 & 0 & 0 & 0 \\ 0 & 0 & \gamma_h & z_{44} & 0 & 0 & 0 \\ 0 & 0 & -\beta_m(T^*,R^*)\frac{\Phi(T^*,R^*)}{\mu_m} & 0 & z_{55} & 0 & 0 \\ 0 & 0 & \beta_m(T^*,R^*)\frac{\Phi(T^*,R^*)}{\mu_m} & 0 & 0 & z_{66} & 0 \\ 0 & 0 & 0 & 0 & 0 & \alpha_m & z_{77} \end{pmatrix}, \tag{22}$$

where $z_{11} = -\mu_h$, $z_{22} = -(\alpha_h + \mu_h)$, $z_{33} = -(\mu_h + \delta + \gamma_h)$, $z_{44} = -(\mu_h + \omega_h)$, $z_{55} = -\mu_m$, $z_{66} = -(\alpha_m + \mu_m)$, $z_{77} = -\mu_m$.

Setting $c_1 = \alpha_h + \mu_h$, $c_2 = \mu_h + \delta + \gamma_h$, $c_3 = \alpha_m + \mu_m$, $c_4 = \mu_m$ and from the equation (22) the Jacobian matrix obtained as the polynomial function given by

$$(-\lambda-\mu_h)(-\lambda-\mu_m)(-\lambda-(\omega_h+\mu_h))\left(\lambda^4 + b_1\lambda^3 + b_2\lambda^2 + b_3\lambda + b_4\right) = 0 \tag{23}$$

where

$$b_1 = c_1 + c_2 + c_3 + c_4, \tag{24}$$

$$b_2 = c_1c_2 + c_2c_3 + 2c_1c_4 + c_3c_4 + c_2c_4, \tag{25}$$

$$b_3 = 2c_1c_2c_3 + c_1c_2c_4 + c_2c_3c_4, \tag{26}$$

$$b_4 = c_1c_2c_3c_4 - \frac{\beta_h(T^*,R^*)\Psi\beta_m(T^*,R^*)\Phi(T^*,R^*)\alpha_h\alpha_m}{\mu_m\mu_h}. \tag{27}$$

From equation (23), we obtain

$$\lambda_1 = -\mu_h < 0, \lambda_2 = -\mu_m < 0, \lambda_3 = -(\omega_h + \mu_h) < 0, \tag{28}$$

and we get from the final polynomial equation,

$$\lambda^4 + b_1\lambda^3 + b_2\lambda^2 + b_3\lambda + b_4 = 0. \tag{29}$$

Using the Routh-Hurwitz criteria [20, 21], we can see that all of the equation's eigenvalues (29) have negative roots or imaginary roots with a negative real part if

$$\begin{aligned} &b_1 > 0, b_2 > 0, b_3 > 0, b_4 > 0, b_1b_2 - b_3 > 0, b_1b_2b_3 - b_3^2 \\ &> 0, b_1b_2b_3 - b_3^2 - b_4b_1^2 > 0. \end{aligned} \tag{30}$$

Clearly, we have seen that $b_1 > 0, b_2 > 0$, and $b_3 > 0$, because they are a sum of positive parameters and at $T^* = T_{\max}$ the value of b_4 is described by

$$\begin{aligned} b_4 &= \mu_m(\gamma_h+\delta+\mu_h)(\alpha_h+\mu_h)(\alpha_m+\mu_m) \\ &\quad - \frac{(\beta_{0h}+\beta_{2h})\Psi(\beta_{0m}+\beta_{2m})(\Phi_0+\Phi_{2m})\alpha_h\alpha_m}{\mu_m\mu_h} = 1 - \mathfrak{R}_{02}^2. \end{aligned} \tag{31}$$

However, for b_4 to be positive, $1 - \mathfrak{R}_{02}^2$ must also be positive, resulting in $\mathfrak{R}_{02} < 1$. Furthermore, when $\mathfrak{R}_{02} > 1$, then, $b_4 < 0$, implying that disease-free equilibrium (DFE) is unstable. As a result, since $\mathfrak{R}_{01} < \mathfrak{R}_{02}$, the DFE is locally asymptotically stable in Ω if $\mathfrak{R}_{01} < \mathfrak{R}_{02} < 1$. □

3.5. Global Stability of Disease-Free Equilibrium

Theorem 3. *If $\mathfrak{R}_{01} < \mathfrak{R}_{02} < 1$; then, the disease free-equilibrium point(s) of the system (1) is globally asymptotically stable in Ω.*

Proof. We used the technique implemented by Lyapunov theorem [19]; first, we developed the following Lyapunov function defined as

$$\begin{aligned} M &= \left(\frac{\alpha_h}{(\alpha_h+\mu_h)(\mu_h+\delta+\gamma_h)}\right)E_h + \left(\frac{I_h}{\mu_h+\delta+\gamma_h}\right) \\ &\quad + \left(\frac{\mu_m\mathfrak{R}_{02}}{\beta_{3m}\Phi_{3m}}\right)E_m + \left(\frac{\mu_m(\alpha_m+\mu_m)\mathfrak{R}_{02}}{\beta_{3m}\Phi_{3m}\alpha_m}\right)I_m. \end{aligned} \tag{32}$$

Then differentiating the Lyapunov function with respect

to time t, the obtained result is given by

$$\begin{aligned}\frac{dM}{dt} &= \left(\frac{\alpha_h}{(\alpha_h+\mu_h)(\mu_h+\delta+\gamma_h)}\right)\frac{dE_h}{dt} + \left(\frac{1}{\mu_h+\delta+\gamma_h}\right)\frac{dI_h}{dt} \\ &\quad + \left(\frac{\mu_m\mathfrak{R}_{02}}{\beta_{3m}\Phi_{3m}}\right)\frac{dE_m}{dt} + \left(\frac{\mu_m(\alpha_m+\mu_m)\mathfrak{R}_{02}}{\beta_{3m}\Phi_{3m}\alpha_m}\right)\frac{dI_m}{dt}, \\ &= \left(\frac{\alpha_h}{(\alpha_h+\mu_h)(\mu_h+\delta+\gamma_h)}\right)(\beta_{3h}S_hI_m - (\mu_h+\alpha_h)E_h) \\ &\quad + \left(\frac{1}{\mu_h+\delta+\gamma_h}\right)(\alpha_hE_h - (\mu_h+\delta+\gamma_h)I_h) \\ &\quad + \left(\frac{\mu_m\mathfrak{R}_{02}}{\beta_{3m}\Phi_{3m}}\right)(\beta_{3m}S_mI_h - (\mu_m+\alpha_m)E_m) \\ &\quad + \left(\frac{\mu_m(\alpha_m+\mu_m)\mathfrak{R}_{02}}{\beta_{3m}\Phi_{3m}\alpha_m}\right)(\alpha_mE_m - \mu_m)I_m, \\ &= \frac{\beta_{3h}\alpha_hS_hI_m}{(\alpha_h+\mu_h)(\mu_h+\delta+\gamma_h)} - I_h + \frac{\mu_mS_mI_h\mathfrak{R}_{02}}{\Phi_{3m}} \\ &\quad - \left(\frac{\mu_m^2(\alpha_m+\mu_m)\mathfrak{R}_{02}I_m}{\beta_{3m}\alpha_m\Phi_{3m}}\right), \\ &\le \left(\frac{\beta_{3h}\alpha_h\Psi}{(\alpha_h+\mu_h)(\mu_h+\delta+\gamma_h)\mu_h} - \frac{\mu_m^2(\alpha_m+\mu_m)\mathfrak{R}_{02}}{\beta_{3m}\alpha_m\Phi_{3m}}\right)I_m + (\mathfrak{R}_{02}-1)I_h, \\ &= \left[\left(\sqrt{\frac{(\beta_{3h}\alpha_h\Psi)\mu_m^2(\alpha_m+\mu_m)}{(\alpha_h+\mu_h)(\mu_h+\delta+\gamma_h)\mu_h(\beta_{3m}\alpha_m\Phi_{3m})}}\right)I_m + I_h\right](\mathfrak{R}_{02}-1),\end{aligned} \tag{33}$$

where $\beta_{3h} = \beta_{0h} + \beta_{2h}, \beta_{3m} = \beta_{0m} + \beta_{2m}$, and $\Phi_{3m} = \Phi_0 + \Phi_{2m}$.

Obviously, $dM/dt < 0$ if $\mathfrak{R}_{02} < 1$ and $dM/dt = 0$ iff $E_h = 0, I_h = 0, E_m = 0, I_m = 0$. This demonstrates that the dominant compact invariant set in $\{(S_h, E_h, I_h, R_h, S_m, E_m, I_m) \in \Omega : dM/dt = 0\}$ represents the singleton set DFE in Ω. As a result of LaSalle's invariant principle [22], every solution which begins in the region approaches DFE as t (time) tends to infinity. Since $\mathfrak{R}_{01} < \mathfrak{R}_{02}$, the DFE is globally asymptotically stable in Ω if $\mathfrak{R}_{01} < \mathfrak{R}_{02} < 1$. □

3.6. Malaria Present Equilibrium. The endemic equilibrium point $E^* = (S_h^*, E_h^*, I_h^*, R_h^*, S_m^*, E_m^*, I_m^*, T^*, R^*)$ is the condition in which malaria is found in the human population, which can be obtained by equating all the model equations of system (1) to zero. At this point, let $\lambda_h^* = \beta_h(T^*, R^*)I_m^*$ and $\lambda_m^* = \beta_m(T^*, R^*)I_h^*$ be force of infection of human and mosquito, respectively, and from the system (1), the endemic equilibrium point at $(T^*, R^*) = (T_0, R_0)$ is provided by

$$S_h^* = \frac{\Psi(\alpha_h+\mu_h)(\mu_h+\delta+\gamma_h)(\mu_h+\omega_h)}{(\alpha_h+\mu_h)(\mu_h+\delta+\gamma_h)(\mu_h+\omega_h)(\lambda_h^*+\mu_h) - (\omega_h\alpha_h\gamma_h\lambda_h^*)}, \tag{34}$$

$$E_h^* = \frac{\Psi(\mu_h+\delta+\gamma_h)(\mu_h+\omega_h)\lambda_h^*}{(\alpha_h+\mu_h)(\mu_h+\delta+\gamma_h)(\mu_h+\omega_h)(\lambda_h^*+\mu_h) - (\omega_h\alpha_h\gamma_h\lambda_h^*)}, \tag{35}$$

$$I_h^* = \frac{\Psi\alpha_h(\mu_h+\omega_h)\lambda_h^*}{(\alpha_h+\mu_h)(\mu_h+\delta+\gamma_h)(\mu_h+\omega_h)(\lambda_h^*+\mu_h) - (\omega_h\alpha_h\gamma_h\lambda_h^*)}, \tag{36}$$

$$R_h^* = \frac{\Psi\alpha_h\gamma_h\lambda_h^*}{(\alpha_h+\mu_h)(\mu_h+\delta+\gamma_h)(\mu_h+\omega_h)(\lambda_h^*+\mu_h) - (\omega_h\alpha_h\gamma_h\lambda_h^*)}, \tag{37}$$

$$S_m^* = \frac{\Phi_0}{\lambda_m^*+\mu_m}, \tag{38}$$

$$E_m^* = \frac{\lambda_m^*\Phi_0}{(\lambda_m^*+\mu_m)(\alpha_m+\mu_m)}, \tag{39}$$

$$I_m^* = \frac{\lambda_m^*\alpha_m\Phi_0}{(\lambda_m^*+\mu_m)(\alpha_m+\mu_m)\mu_m}. \tag{40}$$

By substituting I_h^* and I_m^* from equation (34) into λ_m^* and λ_h^*, respectively, and λ_h^* is obtained by solving the equation

$$A_1(\lambda_h^*)^2 + B_1(\lambda_h^*) = 0, \tag{41}$$

where

$$\begin{aligned}A_1 &= \mu_m(\alpha_m+\mu_m)[\beta_{0m}\alpha_h\Psi(\mu_h+\omega_h) \\ &\quad + \mu_m((\mu_h+\delta+\gamma_h)(\alpha_h+\mu_h)(\mu_h+\omega_h)) - \mu_m(\omega_h\gamma_h\alpha_h)],\end{aligned} \tag{42}$$

$$B_1 = (\omega_h+\mu_h)\left[\mu_h\mu_m^2(\alpha_h+\mu_h)(\alpha_m+\mu_m)(\mu_h+\delta+\gamma_h)\left(1-\mathfrak{R}_{01}^2\right)\right]. \tag{43}$$

Therefore, $A_1 > 0$ and $B_1 > 0$ whenever $\mathfrak{R}_{01} < 1$, so that $\lambda_h^* = -B_1/A_1 < 0$. As a result, positive endemic equilibrium does not occur when $\mathfrak{R}_{01} < 1$. This shows that endemic equilibrium is found if B is less than zero which means that there is endemic equilibrium for the model. Similarly, applying the same procedure, the endemic equilibrium point the model (1) with $(T^*, R^*) = (T_{\max}, R_{\max})$ is described in the following as obtain:

$$S_h^* = \frac{\Psi(\alpha_h+\mu_h)(\mu_h+\delta+\gamma_h)(\mu_h+\omega_h)}{(\alpha_h+\mu_h)(\mu_h+\delta+\gamma_h)(\mu_h+\omega_h)(\lambda_h^*+\mu_h) - (\omega_h\alpha_h\gamma_h\lambda_h^*)}, \tag{44}$$

$$E_h^* = \frac{\Psi(\mu_h+\delta+\gamma_h)(\mu_h+\omega_h)\lambda_h^*}{(\alpha_h+\mu_h)(\mu_h+\delta+\gamma_h)(\mu_h+\omega_h)(\lambda_h^*+\mu_h) - (\omega_h\alpha_h\gamma_h\lambda_h^*)}, \tag{45}$$

$$I_h^* = \frac{\Psi\alpha_h(\mu_h+\omega_h)\lambda_h^*}{(\alpha_h+\mu_h)(\mu_h+\delta+\gamma_h)(\mu_h+\omega_h)(\lambda_h^*+\mu_h) - (\omega_h\alpha_h\gamma_h\lambda_h^*)}, \tag{46}$$

$$R_h^* = \frac{\Psi\alpha_h\gamma_h\lambda_h^*}{(\alpha_h+\mu_h)(\mu_h+\delta+\gamma_h)(\mu_h+\omega_h)(\lambda_h^*+\mu_h) - (\omega_h\alpha_h\gamma_h\lambda_h^*)}, \tag{47}$$

$$S_m^* = \frac{(\Phi_0+\Phi_{2m})}{\lambda_m^*+\mu_m}, \tag{48}$$

$$E_m^* = \frac{\lambda_m^*(\Phi_0+\Phi_{2m})}{(\lambda_m^*+\mu_m)(\alpha_m+\mu_m)}, \tag{49}$$

$$I_m^* = \frac{\lambda_m^* \alpha_m (\Phi_0 + \Phi_{2m})}{(\lambda_m^* + \mu_m)(\alpha_m + \mu_m)\mu_m}. \tag{50}$$

Similarly, substituting I_h^* and I_m^* from equation (44) into λ_m^* and λ_h^*, respectively, and λ_h^* is obtained by solving the equation

$$C(\lambda_h^*)^2 + D(\lambda_h^*) = 0, \tag{51}$$

where

$$C = \mu_m(\alpha_m + \mu_m)[(\beta_{0m} + \beta_{2m})\alpha_h \Psi(\mu_h + \omega_h) + \mu_m((\mu_h + \delta + \gamma_h)(\alpha_h + \mu_h)(\mu_h + \omega_h)) - \mu_m(\omega_h \gamma_h \alpha_h)], \tag{52}$$

$$D = (\omega_h + \mu_h)\left[\mu_h \mu_m^2 (\alpha_h + \mu_h)(\alpha_m + \mu_m)(\mu_h + \delta + \gamma_h)\left(1 - \mathfrak{R}_{02}^2\right)\right]. \tag{53}$$

As a result of equation (21), if $\mathfrak{R}_{02} < 1$, it follows that $\mathfrak{R}_{01} < 1$ exists, and DFE exists for both $\mathfrak{R}_{01}$ and $\mathfrak{R}_{02}$. However, $\mathfrak{R}_{01} < 1$ does not automatically imply $\mathfrak{R}_{02} < 1$, because the value of $\mathfrak{R}_{02}$ can be greater than 1, implying that $\mathfrak{R}_{02}$ may present backward bifurcation while $\mathfrak{R}_{01}$ can only present forward bifurcation.

4. Model Parameter Sensitivity Analysis

Malaria eradication strategies should focus on key parameters that have a significant impact on the basic reproduction number. The parameters found in the model (1) influence the basic reproduction number. Because those parameters can increase or decrease a basic reproduction number ($\mathfrak{R}_0$) as their values change, and vice versa. The sensitivity analysis is used to identify the parameters that have a large influence on the basic reproduction number ($\mathfrak{R}_0$). To perform the sensitivity analysis, the method described in [23–25] is used.

Definition 4 (see [23, 24]). The normalized forward sensitivity index of $\mathfrak{R}_0$ that differentiable with respect to a given parameter Q is defined as

$$\tau_Q^{\mathfrak{R}_0} = \frac{\partial \mathfrak{R}_0}{\partial Q} \times \frac{Q}{\mathfrak{R}_0}, \tag{54}$$

for Q describes the basic parameters.

For example, the sensitivity index of $\mathfrak{R}_{01}$ with respect to basic parameter β_{0m} is obtained as

$$\tau_{\beta_{0m}}^{\mathfrak{R}_{01}} = \frac{\partial \mathfrak{R}_{01}}{\partial \beta_{0m}} \times \frac{\beta_{0m}}{\mathfrak{R}_{01}}, = \frac{1}{2\sqrt{\beta_{0h}\Psi\beta_{0m}\Phi_0\alpha_h\alpha_m/\mu_h\mu_m^2(\mu_h + \delta + \gamma_h)(\alpha_h + \mu_h)(\alpha_m + \mu_m)}} \times \frac{\beta_{0h}\Phi_0\Psi\alpha_h\alpha_m}{\mu_h\mu_m^2(\mu_h + \delta + \gamma_h)(\alpha_h + \mu_h)(\alpha_m + \mu_m)} \times \frac{\beta_{0m}}{\mathfrak{R}_{01}} = \frac{1}{2} > 0. \tag{55}$$

Using a similar procedure for the remaining parameters, $\tau_{\beta_{0m}}^{\mathfrak{R}_{01}}, \tau_{\Psi}^{\mathfrak{R}_{01}}, \tau_{\Phi_0}^{\mathfrak{R}_{01}}, \tau_{\mu_h}^{\mathfrak{R}_{01}}, \tau_{\mu_m}^{\mathfrak{R}_{01}}, \tau_{\delta}^{\mathfrak{R}_{01}}, \tau_{\gamma_h}^{\mathfrak{R}_{01}} \tau_{\alpha_h}^{\mathfrak{R}_{01}}, \tau_{\alpha_m}^{\mathfrak{R}_{01}}$ are obtained, and their sensitivity indices are shown in Table 2 as follows.

Table 2: Sensitivity indices of parameters.

Parameter symbol	Sensitivity index
α_h	0.002346
α_m	0.248098
Ψ	0.5
Φ_0	0.5
β_{0h}	0.5
β_{0m}	0.5
μ_m	-0.023650
μ_h	-0.540314
δ	-0.485258
γ_h	-0.026464

The sensitivity index of $\mathfrak{R}_{02}$ with respect to parameters is obtained using a similar method, and their sensitivity indices are written in Table 3.

4.1. Expression of the Sensitivity Indices. The sensitivity analysis description of a basic reproductive number $\mathfrak{R}_{01}$ with respect to ten basic parameters was stated in the Table 2. We can conclude that the parameters $\alpha_m, \alpha_h, \Psi, \Phi_0, \beta_{0h}$, and β_{0m} with positive sensitivity indices will increase the value of $\mathfrak{R}_{01}$ if their values increase while the other parameters remain constant. This demonstrates that the population's infection rate is increasing as a result of secondary cases. In contrast, the basic parameters μ_m, μ_h, δ, and γ_h with negative indices decrease the value of $\mathfrak{R}_{01}$ if their value increases while retaining the constant of rest parameters. For example, $\tau_{\beta_{0m}}^{\mathfrak{R}_{01}} == 0.5$ shows that decreasing (increasing) the mosquito contact rate by 10% reduces (increases) the $\mathfrak{R}_{01}$ by 5%. Similarly, $\tau_{\mu_m}^{\mathfrak{R}_{01}} = -0.023650$ and indicates that decreasing (increasing) the mosquito death rate by 10% increases (decreases) the basic reproduction number $\mathfrak{R}_{01}$ by 0.23650%. Also, the sensitivity analysis expression of the basic reproductive number $\mathfrak{R}_{02}$ with respect to thirteen basic parameters was shown in Table 3. As a result, the parameters $\alpha_m, \alpha_h, \Psi, \Phi_0, \Phi_{1m}, \beta_{0h}\beta_{1h}, \beta_{0m}$, and β_{1m} have positive sensitivity indices. They will have a large influence on the spread of the malaria disease in the population. Because the transmission of malaria disease increases as their value increases, so does the number of infections as secondary cases in the population. The sensitivity indices for the parameters μ_m, μ_h, δ, and γ_h are all negative. As their values increase, those parameters have the potential to reduce malaria disease transmission while remaining constant. For example, $\tau_{\beta_{0m}}^{\mathfrak{R}_{02}} = 0.385$ indicates that decreasing (increasing) the mosquito contact rate by 10% decreases (increases) the $\mathfrak{R}_{02}$ by 3.85%. In contrast, $\tau_{\mu_m}^{\mathfrak{R}_{02}} = -0.023650$ demonstrates that decreasing (increasing) the mosquito death rate by 10% increases (decreases) the basic reproduction number $\mathfrak{R}_{02}$ by 0.23650%.

Table 3: Sensitivity indices of parameters.

Parameter symbol	Sensitivity index
α_h	0.020346
α_m	0.238096
Ψ	0.5
Φ_0	0.082438
β_{0h}	0.321659
β_{0m}	0.385000
Φ_{1m}	0.068169
β_{1h}	0.208341
β_{1m}	0.214286
μ_m	-0.013650
μ_h	-0.500314
δ	-0.476258
γ_h	-0.026464

5. Optimal Control Model

In this section, we provide a thorough qualitative examination of the time-dependent malaria dynamic model (1). The Pontryagin's maximum principle [28] is used to describe this analysis, with the goal of lowering the exposed human $E_h(t)$, infected human $I_h(t)$, infected mosquito $I_m(t)$, and control costs $u_i(t)$. In the case of time-dependent control, we employ Pontryagin's maximum principle to derive the necessary conditions for disease control. After incorporating the controls into the malaria transmission model (1), the optimal control problem is as follows:

$$\begin{cases} \dfrac{dS_h}{dt} = \Psi - (1-u_1)\dfrac{\beta_h(T,R)}{1+z^*I_m}S_hI_m - \mu_hS_h + \omega_hR_h, \\ \dfrac{dE_h}{dt} = (1-u_1)\dfrac{\beta_h(T,R)}{1+z^*I_m}S_hI_m - (\mu_h+\alpha_h)E_h, \\ \dfrac{dI_h}{dt} = \alpha_hE_h - (\mu_h+\delta+\gamma_h+u_2)I_h, \\ \dfrac{dR_h}{dt} = (\gamma_h+u_2)I_h - (\mu_h+\omega_h)R_h, \\ \dfrac{dS_m}{dt} = \Phi(T,R) - (1-u_1)\dfrac{\beta_m(T,R)}{1+m^*I_h}S_mI_h - (\mu_m+u_3)S_m, \\ \dfrac{dE_m}{dt} = (1-u_1)\dfrac{\beta_m(T,R)}{1+m^*I_h}S_mI_h - (\mu_m+\alpha_m+u_3)E_m, \\ \dfrac{dI_m}{dt} = \alpha_mE_m - (\mu_m+u_3)I_m, \\ \dfrac{dT}{dt} = r\left(1-\dfrac{T}{T_{\max}}\right)(T-T_0), \\ \dfrac{dR}{dt} = \mathrm{m}\dfrac{dT}{dt} \Rightarrow R(t) = \mathrm{m}(T(t)-T_0) + \varepsilon, \end{cases} \tag{56}$$

where $u_1(t)$ represents protective control using treated bed net, $u_2(t)$ represents antimalaria drug treatment control, and $u_3(t)$ denotes mosquito control via indoor residual spraying. The objective functional (57) of the optimal control problem (56) is given by

$$J(u_1,u_2,u_3) = \underbrace{\min}_{u_1,u_2,u_3} \int_0^{t_f} \cdot \left(D_1E_h + D_2I_h + D_3I_m + \frac{1}{2}\left(B_1u_1^2 + B_2u_2^2 + B_3u_3^2\right)\right)dt, \tag{57}$$

where t_f represents the final time of control implementation, and quantities D_1, D_2, and D_3 are weights constants of the exposed human population, infected human population, and infected mosquito population, respectively, while B_1, B_2, and B_3 are weight constants used for treated bed net, treatment control using antimalaria drugs, and indoor residual spraying. In this paper, we make the expression $1/2B_iu_i^2$ for the cost-control functions to be quadratic in order to obtain a unique optimal expression for each of the control variables from the optimality condition as in other studies [29–34]. The main goal is to achieve the best control triple u_1^*, u_2^*, and u_3^* so that

$$J(u_1^*,u_2^*,u_3^*) = \min\{J(u_1,u_2,u_3): u_1,u_2,u_3 \in U\}, \tag{58}$$

where $U = (u_1,u_2,u_3)$: $u_i(t)$ such that u_1, u_2, and u_3 are Lebesgue measurable on $t \in [0,t_f]$ with $0 \le u_i(t) \le 1$, for $i = 1$, 2, 3 is the control set. We express the Hamiltonian (H), which consists of the state equations (56) and integrand of the objective functional (57), by using the Pontryagin's maximum principle [28] to obtain the necessary condition.

$$\begin{aligned} H = {} & \left[D_1E_h + D_2I_h + D_3I_m + \frac{1}{2}\sum_{i=1}^{3}B_iu_i^2\right] \\ & + \lambda_i\left[\frac{dS_h}{dt} + \frac{dE_h}{dt} + \frac{dI_h}{dt} + \frac{dR_h}{dt} + \frac{dS_m}{dt}\right. \\ & \left. + \frac{dE_m}{dt} + \frac{dI_m}{dt} + \frac{dT}{dt} + \frac{dR}{dt}\right], i = 1,\cdots,9. \end{aligned} \tag{59}$$

By plugging the given equations (56) and (57) into a minimizing problem of a Hamiltonian function (H) with respect to controls. The Hamiltonian (59) becomes

$$\begin{aligned} H = {} & \left[B_1E_h + B_2I_h + B_3I_m + \frac{1}{2}\left(D_1u_1^2 + D_2u_2^2 + D_3u_3^2\right)\right] \\ & + \lambda_1\left[\Psi - (1-u_1)\frac{\beta_h(T,R)}{1+z^*I_m}S_hI_m - \mu_hS_h + \omega_hR_h\right] \\ & + \lambda_2\left[(1-u_1)\frac{\beta_h(T,R)}{1+z^*I_m}S_hI_m - (\mu_h+\alpha_h)E_h\right] \end{aligned}$$

$$
\begin{aligned}
&+\lambda_3[\alpha_h E_h-(\mu_h+\delta+\gamma_h+u_2)I_h]\\
&+\lambda_4[(\gamma_h+u_2)I_h-(\mu_h+\omega_h)R_h]\\
&+\lambda_5\left[\Phi(T,R)-(1-u_1)\frac{\beta_m(T,R)}{1+m^*I_h}S_mI_h-(\mu_m+u_3)S_m\right]\\
&+\lambda_6\left[(1-u_1)\frac{\beta_m(T,R)}{1+m^*I_h}S_mI_h-(\mu_m+\alpha_m+u_3)E_m\right]\\
&+\lambda_7[\alpha_mE_m-(\mu_m+u_3)+\lambda_8\left[r\left(1-\frac{T}{T_{\max}}\right)(T-T_0)\right]\\
&+\lambda_9\left[mr\left(1-\frac{T}{T_{\max}}\right)(T-T_0)\right],
\end{aligned}
\tag{60}
$$

where λ_i for $i=1,\cdots,9$ is adjoint variables. Next, we present the adjoint system and control characterizations using Pontryagin's maximum principle [30], in conjunction with the existence of the optimal control problem [35], the following result can be obtained.

Theorem 5. *Suppose we have an optimal control set* $u^*=(u_1^*,u_2^*,u_3^*)$ *and* $(S_h^*,E_h^*,I_h^*,R_h^*,S_m^*,E_m^*,I_m^*,T^*,R^*)$ *solutions of the respective state system (56) that minimize* $J(u_1,u_2,u_3)$ *over U; then, there exist costate variables* $\lambda_1,\lambda_2,\lambda_3,\lambda_4,\lambda_5,\lambda_6,\lambda_7,\lambda_8$, *and* λ_9 *such that*

$$
\begin{cases}
\dfrac{d\lambda_1}{dt}=-\left((1-u_1)\dfrac{\beta_h(T,R)}{1+z^*I_m}I_m(\lambda_2-\lambda_1)\right)+\mu_h\lambda_1,\\
\dfrac{d\lambda_2}{dt}=-D_1+\lambda_2(\mu_h+\alpha_h)-\alpha_h\lambda_3,\\
\dfrac{d\lambda_3}{dt}=-D_2-\left((1-u_1)\dfrac{\beta_m(T,R)}{1+m^*I_h}S_m(\lambda_6-\lambda_5)\right)+\lambda_3(\mu_h+\delta+\gamma_h+u_2)-\lambda_4(u_2+\gamma_h),\\
\dfrac{d\lambda_4}{dt}=-\omega_h\lambda_1+\lambda_4(\mu_h+\omega_h),\\
\dfrac{d\lambda_5}{dt}=-\left((1-u_1)\dfrac{\beta_m(T,R)}{1+m^*I_h}I_h(\lambda_6-\lambda_5)\right)+\lambda_5(u_3+\mu_m),\\
\dfrac{d\lambda_6}{dt}=\lambda_6(u_3+\mu_m+\alpha_m)-\lambda_7\alpha_m,\\
\dfrac{d\lambda_7}{dt}=-D_3-\left((1-u_1)\dfrac{\beta_h(T,R)}{1+z^*I_m}S_h(\lambda_2-\lambda_1)\right)+\lambda_7(u_3+\mu_m),\\
\dfrac{d\lambda_8}{dt}=-r\lambda_8-r\lambda_8\left(\dfrac{T_0}{T_{\max}}-\dfrac{2T}{T_{\max}}\right),\\
\dfrac{d\lambda_9}{dt}=-mr\lambda_9-mr\lambda_9\left(\dfrac{T_0}{T_{\max}}-\dfrac{2T}{T_{\max}}\right).
\end{cases}
\tag{61}
$$

with full time (transversality) conditions

$$
\begin{aligned}
\lambda_1(t_f)=\lambda_2(t_f)=\lambda_3(t_f)=\lambda_4(t_f)=\lambda_5(t_f)=\lambda_6(t_f)\\
=\lambda_7(t_f)=\lambda_8(t_f)=\lambda_9(t_f)=0.
\end{aligned}
\tag{62}
$$

Moreover, the optimal controls u_1^*,u_2^*,u_3^* *with the optimality condition are represented by*

$$
u_1^*=\max\left\{0,\min\left\{1,\frac{(\lambda_2-\lambda_1)(\beta_h(T,R)/1+z^*I_m)S_h^*I_m^*+(\lambda_6-\lambda_5)(\beta_m(T,R)/1+m^*I_h)S_m^*I_h^*}{B_1}\right\}\right\},
\tag{63}
$$

$$
u_2^*=\max\left\{0,\min\left\{1,\frac{(\lambda_3-\lambda_4)I_h^*}{B_2}\right\}\right\},
\tag{64}
$$

$$
u_3^*=\max\left\{0,\min\left\{1,\frac{(\lambda_5S_m^*+\lambda_6E_m^*+\lambda_7I_m^*)}{B_3}\right\}\right\}.
\tag{65}
$$

Proof. Differentiate the Hamiltonian function H (??) with respect to the state variables $S_h,E_h,I_h,R_h,S_m,E_m,I_m,T$, and R, respectively, the adjoint equations stated at the system (61) are obtained. Thus, the adjoint equations are given by

$$
\begin{cases}
\dfrac{d\lambda_1}{dt}=-\dfrac{\partial H}{\partial S_h}=-\left((1-u_1)\dfrac{\beta_h(T,R)}{1+z^*I_m}I_m(\lambda_2-\lambda_1)\right)+\mu_h\lambda_1,\\
\dfrac{d\lambda_2}{dt}=-\dfrac{\partial H}{\partial E_h}=-D_1+\lambda_2(\mu_h+\alpha_h)-\alpha_h\lambda_3,\\
\dfrac{d\lambda_3}{dt}=-\dfrac{\partial H}{\partial I_h}=-D_2-\left((1-u_1)\dfrac{\beta_m(T,R)}{1+m^*I_h}S_m(\lambda_6-\lambda_5)\right)+\lambda_3(\mu_h+\delta+\gamma_h+u_2)-\lambda_4(u_2+\gamma_h),\\
\dfrac{d\lambda_4}{dt}=-\dfrac{\partial H}{\partial R_h}=-\omega_h\lambda_1+\lambda_4(\mu_h+\omega_h),\\
\dfrac{d\lambda_5}{dt}=-\dfrac{\partial H}{\partial S_m}=-\left((1-u_1)\dfrac{\beta_m(T,R)}{1+m^*I_h}I_h(\lambda_6-\lambda_5)\right)+\lambda_5(u_3+\mu_m),\\
\dfrac{d\lambda_6}{dt}=-\dfrac{\partial H}{\partial E_m}=\lambda_6(u_3+\mu_m+\alpha_m)-\lambda_7\alpha_m,\\
\dfrac{d\lambda_7}{dt}=-\dfrac{\partial H}{\partial I_m}=-D_3-\left((1-u_1)\dfrac{\beta_h(T,R)}{1+z^*I_m}S_h(\lambda_2-\lambda_1)\right)+\lambda_7(u_3+\mu_m),\\
\dfrac{d\lambda_8}{dt}=-\dfrac{\partial H}{\partial T}=-r\lambda_8-r\lambda_8\left(\dfrac{T_0}{T_{\max}}-\dfrac{2T}{T_{\max}}\right),\\
\dfrac{d\lambda_9}{dt}=-\dfrac{\partial H}{\partial R}=-\mathrm{mr}\lambda_9-\mathrm{mr}\lambda_9\left(\dfrac{T_0}{T_{\max}}-\dfrac{2T}{T_{\max}}\right),
\end{cases}
\tag{66}
$$

with transversality conditions

$$
\begin{aligned}
\lambda_1(t_f)=\lambda_2(t_f)=\lambda_3(t_f)=\lambda_4(t_f)=\lambda_5(t_f)=\lambda_6(t_f)\\
=\lambda_7(t_f)=\lambda_8(t_f)=\lambda_9(t_f)=0.
\end{aligned}
\tag{67}
$$

Further, the optimality conditions with respect to the controls are given by

$$
\frac{\partial H}{\partial u_i}=0,\ \text{for } i=1,2,3.
\tag{68}
$$

Using optimality condition (68), the control variables are obtained as

$$
\begin{cases}
u_1^*=\dfrac{(\lambda_2-\lambda_1)(\beta_h(T,R)/1+z^*I_m)S_h^*I_m^*+(\lambda_6-\lambda_5)(\beta_m(T,R)/1+m^*I_h)S_m^*I_h^*}{B_1},\\
u_2^*=\dfrac{(\lambda_3-\lambda_4)I_h^*}{B_2},\\
u_3^*=\dfrac{(\lambda_5S_m^*+\lambda_6E_m^*+\lambda_7I_m^*)}{B_3}.
\end{cases}
\tag{69}
$$

Finally, the compact form with boundary condition, the controls in equation (69), becomes

$$u_1^* = \max\left\{0, \min\left\{1, \frac{(\lambda_2 - \lambda_1)(\beta_h(T,R)/1 + z^* I_m)S_h^* I_m^* + (\lambda_6 - \lambda_5)(\beta_m(T,R)/1 + m^* I_h)S_m^* I_h^*}{B_1}\right\}\right\}, \tag{70}$$

$$u_2^* = \max\left\{0, \min\left\{1, \frac{(\lambda_3 - \lambda_4)I_h^*}{B_2}\right\}\right\}, \tag{71}$$

$$u_3^* = \max\left\{0, \min\left\{1, \frac{(\lambda_5 S_m^* + \lambda_6 E_m^* + \lambda_7 I_m^*)}{B_3}\right\}\right\}. \tag{72}$$

In the next part, we will see the numerical simulation of optimality system to identify an optimum and least cost strategy for controlling the transmission dynamics of malaria. □

6. Numerical Simulation

A numerical result is required in this section to validate the model's analytical result. We use a numerical method to confirm the theoretical results obtained in our model's optimal control model analysis. The optimality system is composed of two systems, the state system (56) and the adjoint system (61), each with its own initial and final-time conditions, with the control value state in equation (62). The iterative method known as the fourth forward-backward Runge-Kutta sweep is used to solve this optimality system. The state equation (56) is solved with the initial values of state variables using the fourth-order forward Runge-Kutta method. We used backward fourth order Runge Kutta to solve the adjoint equations once we had the solution of the state functions and the value of optimal controls. The controls are then updated by a convex combination of the previous controls and the value from the optimality condition (62). This process is repeated, and iterations are completed if the values from previous iterations are close to the values from current iterations [36]. The optimal control problem is simulated with the parameter values given in Table 4 when the basic reproduction numbers are $\mathfrak{R}_{01} = 24.8$ and $\mathfrak{R}_{02} = 56.28$. The initial conditions that we used for simulation of the optimal control are $S_h(0) = 120, E_h(0) = 20, I_h(0) = 10, R_h(0) = 5, S_m(0) = 400, E_m(0) = 60, I_m(0) = 30, T(0) = 16.1^o C$, and $R(0) = 11$ mm. The weight value constants of the state and controls that we used are given as $D_1 = 80, D_2 = 60, D_3 = 100, B_1 = 60, B_2 = 100$, and $B_3 = 80$. To determine the impact of each controls on the reduction of malaria, we used the following four strategies with different combination of two controls at a time and three controls at a time.

6.1. Strategy A. Applying the treated bed net (u_1) and treatment of infected with drugs (u_2).

In this strategy, we used a combination of two controls: protective by treated bed net u_1 and treatment for infected humans with antimalaria drugs u_2 to minimize the objective functional (57), while the control indoor residual spraying u_3 is set to zero. According to Figures 2(a) and 2(b), if there are controls, the total population of exposed and infected humans is lower than if there are no controls, and it tends to be at its lowest value at the end of the intervention. Then, as shown in Figure 2(c), the number of infected mosquitos in the presence of controls is decreasing. In contrast, in the absence of controls, the number of infected mosquitos increases. In order to reduce the number of exposed humans, infected humans, infected mosquito populations, and the associated costs, corresponding with the controls u_1 and u_2, the control profiles shown in Figure 2(d) indicate that use of the treated bed net u_1 maintained its maximum level bound 100 percent for 180 days entire time of strategy and treatment; the infected with antimalaria drugs u_2 is intended upper bound 100 percent for 6 days before gradually declining to zero at the end time.

6.2. Strategy B. Applying the treated bed net (u_1) and indoor residual spraying (u_3).

To reduce the objective functional (57), a combination of two controls protective using treated bed net u_1 and an indoor residual spraying u_3 is implemented, while the control treatment for the infected with antimalaria drugs u_2 is set to zero. Figures 3(a)–3(c) show that using controls reduces the total population of exposed humans, infected humans, and infected mosquitos faster than not using controls. At the end of the intervention, the total number of exposed humans E_h and infected mosquitoes I_m is at its lowest. The profile of the control in Figure 3(d) indicates that the treated bed net u_1 is maintained, it is upper bound at 100% for 178 days before gradually declining to its lower bound and an indoor residual spraying, and u_3 maintains its high level at 100% until 18 days and gradually decreases to its lower bound in the final time.

6.3. Strategy C. Applying the treatment of infected (u_2) and indoor spraying (u_3).

The objective functional (57) is optimized in this strategy by combining two controls treatment of infected with antimalaria drugs u_2 and an indoor residual spraying u_3, whereas the control treated bed net u_1 is set to zero. Figures 4(a) and 4(b) show that in the absence of controls, the significant number of humans exposed and infected is higher than in the presence of controls. At the end of the intervention, the total population of exposed humans E_h and infected humans I_h has reached its lowest point. Figure 4(c) shows that infected mosquitos in the presence of controls are smaller than those in the absence of controls

Table 4: Parameter values from literature used for the model (1).

Parameters	Parameter description	Estimated value	Reference
μ_h	Human death rate due to natural cause	0.00004	[23]
δ	Induced death rate of human	0.068	[23]
γ_h	Recover rate of infected humans	0.0035	[20]
Ψ	Human recruitment rate	0.071	[20]
Φ_0	Mosquito recruitment rate	0.041	[24]
μ_m	Mosquito natural death rate	0.05	[20]
ω_h	Human immune deficiency rate	0.09	[16]
β_{1m}	Mosquito contact rate (incremental)	0.07	[17]
β_{1h}	Human contact rate (incremental)	0.05	[16]
Φ_{1m}	Incremental birth rate of mosquito	0.09	[17]
β_{0h}	Contact rate of human with mosquito	0.03	[23]
β_{0m}	Contact rate of mosquito with human	0.04	[14]
α_h	Exposed human progression rate	0.058	[24]
α_m	Exposed mosquito progression rate	0.055	[24]
m	Temperature dependent rate of precipitation	0.08	[26]
z^*	Percentage of an antibody produced by a human	0.06	[26]
m^*	Percentage of an antibody produced by a mosquito	0.04	[26]
r	Temperature increase rate	0.007	[11]
T_0	The minimum temperature	16°C	[27]
$T_{\max}$	The maximum temperature	28°C	[6]

and fall to the minimum value at the end of the intervention. Similarly, in Figure 4(d), the control profiles show that both antimalaria drug treatment u_2 and indoor residual spraying u_3 maintained their upper bounds of 99 percent for 30 days and 60 days, respectively, before gradually decreasing to their minimum at the end of the intervention.

6.4. Strategy D. Using the treated bed net (u_1), treatment (u_2) and indoor spraying (u_3).

To minimize the objective functional (57), we used all controls protective using treated bed net u_1, treatment for the infected human with antimalaria drugs u_2 and indoor residual spraying u_3. It can be seen in Figures 5(a)–5(c) that the controls indicate that the total population of exposed human, infected human, and infected mosquito populations are increasing in the absence of controls while decreasing in the presence of controls. The total number of exposed humans E_h, infected humans I_h, and infected mosquitos I_m is reduced to their lowest at times $t = 100$, $t = 46$, and $t = 10$, respectively. The control profiles in Figure 5(d) show that with this strategy, the use of the treated bed net u_1 nearly maintained its maximum level 100, and the treatment of an infected human with antimalaria drugs u_2 maintains 100% coverage for 6 days before gradually decreasing to zero, whereas the control, an indoor residual spraying u_3, maintains 100% coverage for 16 days before gradually decreasing to zero at the end of the final time.

Figure 6 illustrates the diagram of bifurcation for the case when $T = T_0$ and $T = T_{\max}$ for the malaria model problem. From this figure, we have seen that the model exhibits forward and backward bifurcation, respectively. The biological meaning of this indicates that in equation (21) if $\mathfrak{R}_{02} < 1$ then automatically implies that $\mathfrak{R}_{01} < 1$ and DFE exist for both $\mathfrak{R}_{01}$ and $\mathfrak{R}_{02}$. However, $\mathfrak{R}_{01} < 1$ does not automatically imply $\mathfrak{R}_{02} < 1$, since the value of $\mathfrak{R}_{02}$ may be greater than 1, which implies that $\mathfrak{R}_{02}$ may present backward bifurcation while $\mathfrak{R}_{01}$ only present forward bifurcation.

7. Cost Effectiveness Analysis

It is critical to identify the most optimal and least expensive strategy, along with a cost-effectiveness analysis, in order to design a method of eradicating malaria transmission. A method known as the incremental cost-effectiveness ratio (ICER) is used to develop such a strategy. Basically, for two strategies say 1 and 2, the ICER will be computed as [37]

$$\frac{\text{Difference in averted costs between two strategies 1 and 2}}{\text{Difference in infections averted bewteen two strategies 1 and 2}}. \quad (73)$$

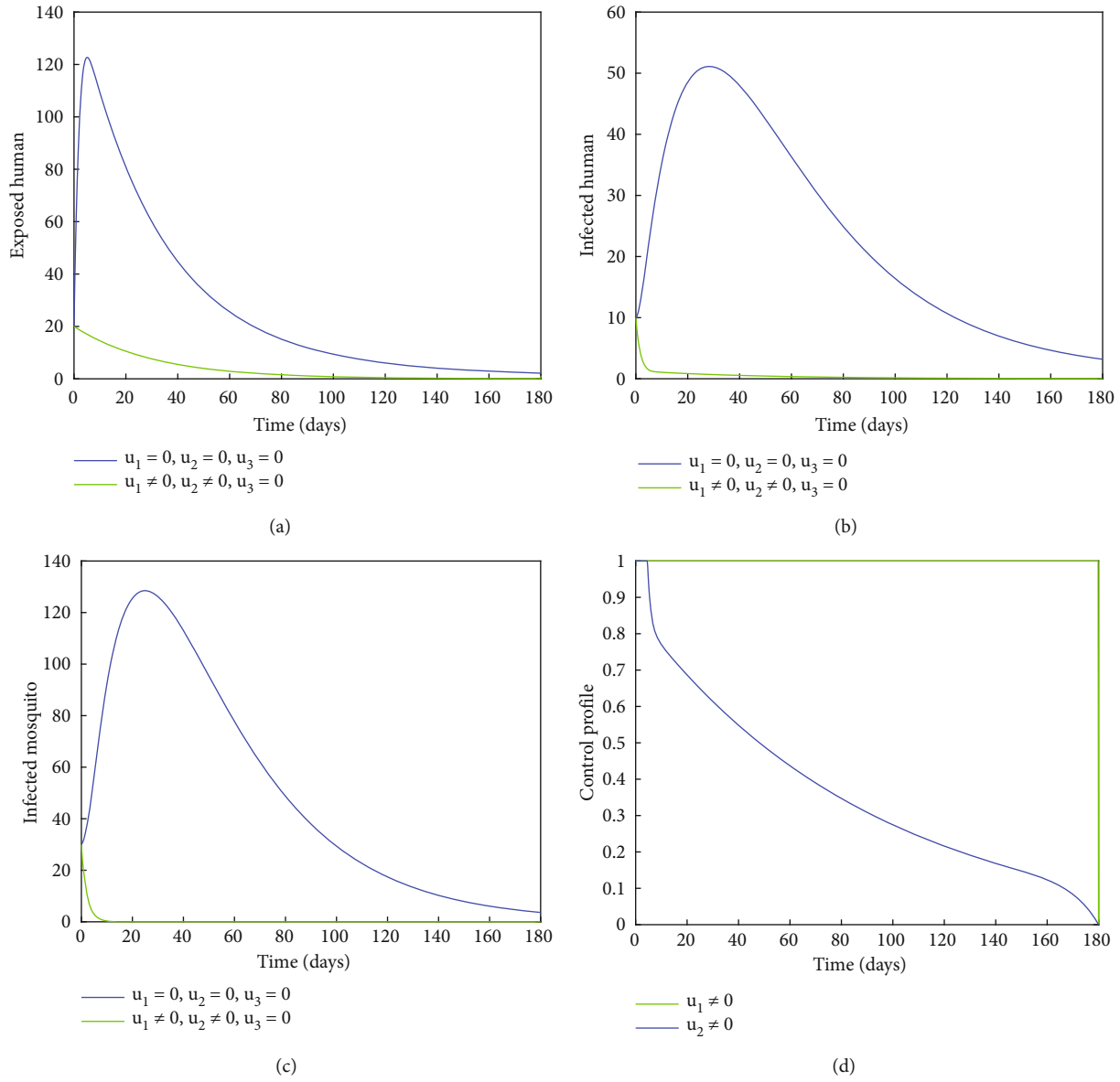

Figure 2: Simulations of model with strategy of treated bed net (u_1) and treatment (u_2).

In this section, the cost-effectiveness of two control strategies, including treated bed nets, antimalaria drug treatment of infected people, and indoor residual spraying, has been calculated. The total number of people averted is calculated by subtracting the total number of new cases of malaria infection with control from the total number of new cases of malaria without control, and the total cost of each strategy is calculated using their respective cost functions $(1/2)B_1u_1^2$, $(1/2)B_2u_2^2$, and $(1/2)B_3u_3^2$, to calculate over the time of intervention [38]. We use the outcome of a numerical simulation from the malaria dynamics model (56) to compute the ICER. However, using only one strategy to prevent the spread of malaria disease in a community may not be effective. Then also from the numerical simulations of the model (56) with the parameters in Table 4, the computed total number of people saved and the total cost in increasing order were shown in Table 5.

After obtaining the total amount of people averted and total cost of each strategy as given in Table 5 to compare two intervention strategies, the incremental cost effectiveness ratio (ICER) for the each competing strategies is estimated as

$$\text{ICER(B)} = \frac{7012.84}{3754.40} = 1.86, \tag{74}$$

$$\text{ICER(C)} = \frac{9098.19 - 7012.84}{4536.24 - 3754.40} = 266.72, \tag{75}$$

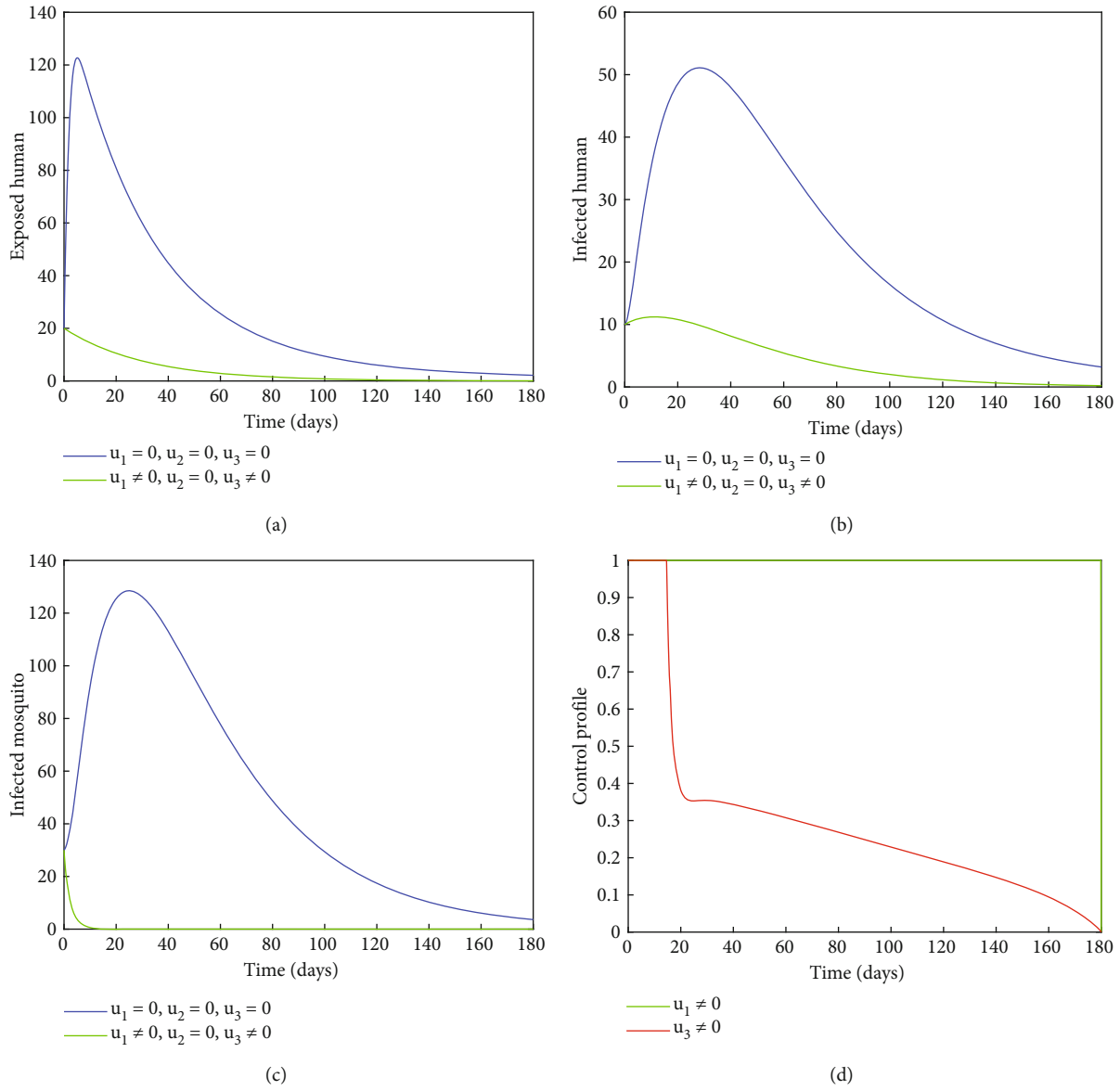

Figure 3: Simulations with strategy of treated bed net (u_1) and indoor spraying (u_3).

$$\text{ICER(A)} = \frac{8306.89 - 99098.19}{4673.34 - 4536.24} = -5.77, \tag{76}$$

$$\text{ICER(D)} = \frac{9154.62 - 8306.89}{4676.62 - 4673.34} = 258.45. \tag{77}$$

The number of people averted in strategy B, C, A, and D in an increasing rank is given in Table 6.

We can see that the ICER(B) is less than the ICER(C) from the strategies B and C in Table 6. This implies that strategy B dominates strategy C. This implies that strategy C is more expensive than strategy C. As a result, we removed C from the strategies. Then, as shown in Table 7, recalculate the ICER for the remaining competing strategies B, A, and D.

The competition between the interventions B and A was depicted in Table 7. As can be seen, ICER(A) is less than ICER(B). This demonstrates that strategy B was dominated by strategy A. As a result, strategy A is more efficient and less expensive than strategy B. As a result, we removed strategy B from the list of competing strategies and recalculated the ICER, as shown in Table 8.

Table 8 compares strategies A and D. This predicts that ICER(D) is greater than ICER(A). This implies that strategy D is dominated by strategy A. As a result, strategy A is the least expensive and most optimal. As a result, we conclude that strategy A, which consists of a combination of treated bed nets and antimalarial drug treatment of infected humans, is the most optimal and

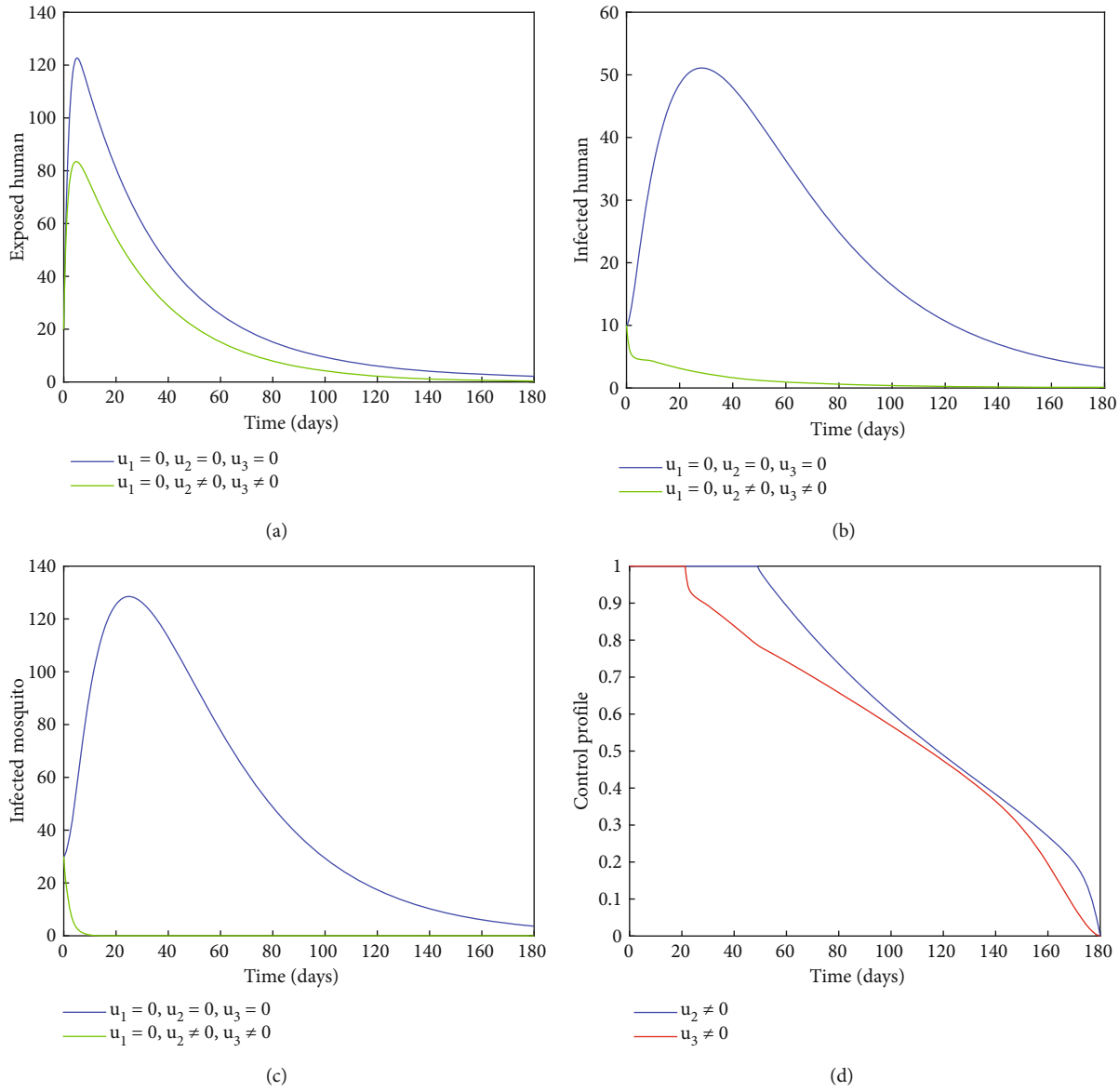

Figure 4: Simulations model with strategy of treatment (u_2) and indoor spraying (u_3).

least expensive strategy for preventing the spread of malaria transmission.

8. Conclusion

We proposed and developed a deterministic malaria transmission dynamic model with climate variability and nonlinear incidence in this paper. Malaria spread is influenced by climate change. The model analysis reveals that it is bounded, epidemiologically meaningful, and mathematically well-posed in a specific domain. Using the next-generation matrix method, we determined the basic reproduction number in relation to the disease-free equilibrium. The Routh-Hurwitz criterion is used to determine local stability of equilibria points, while the Lyapunov function is used to determine global stability. According to the model analysis, if the basic reproduction number is less than one, the disease-free equilibrium is locally and globally asymptotically stable, whereas if the basic reproduction number is greater than one, the unique endemic equilibrium exists. In addition, the sensitivity analysis of the basic reproduction number with respect to all parameters was obtained. The model has a forward and backward bifurcation. Based on the findings, we concluded that reducing human-mosquito contact, increasing mosquito mortality, and increasing the treated rate of infected humans can all help to reduce the malaria burden in the community. Furthermore, the malaria transmission model is extended to an optimal control problem by incorporating three continuous controls, namely, personal protection with treated bed nets, treatment of infected with antimalaria drugs, and indoor residual spraying for vector killing strategy. The maximum principle of

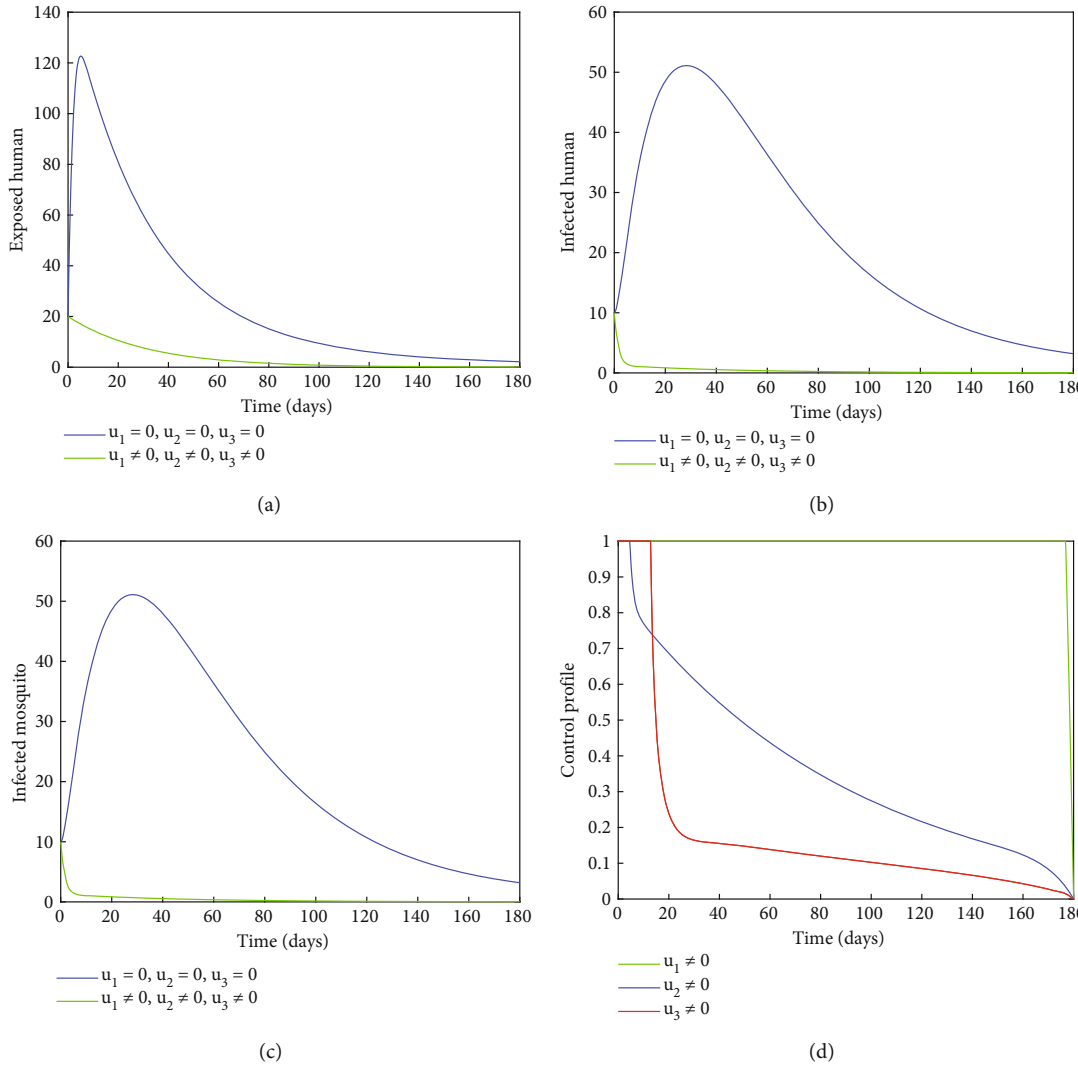

Figure 5: Simulations with strategy of treated bed net (u_1), treatment (u_2), and indoor spraying (u_3).

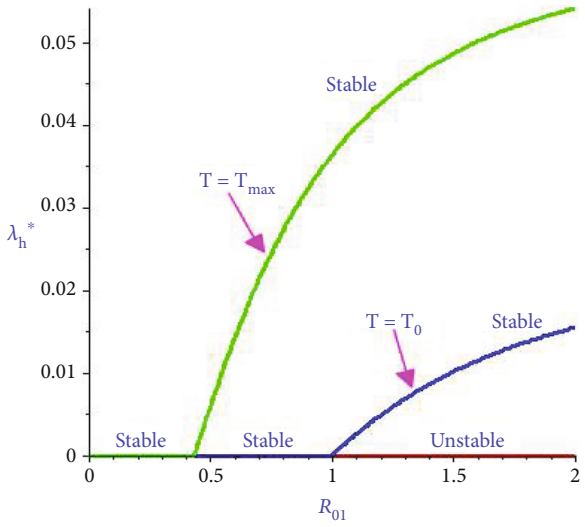

Figure 6: Bifurcation diagrams when $T = T_0$ and $T = T_{max}$ for the malaria model problem.

Table 5: Total amount of infection averted and total cost for all strategies.

Strategies	Total infections averted	Total cost ($)
Strategy B	3754.40	7012.84
Strategy C	4536.24	9098.19
Strategy A	4673.34	8306.89
Strategy D	4676.62	9154.62

Table 6: Total amount of the infection averted and total cost with their ICER.

Strategies	Total infections averted	Total cost ($)	ICER
Strategy B	3754.40	7012.84	1.86
Strategy C	4536.24	9098.19	266.72
Strategy A	4673.34	8306.89	-5.77
Strategy D	4676.62	9154.62	258.45

Table 7: Total amount of the infection averted and total cost with their ICER.

Strategies	Total infections averted	Total cost ($)	ICER
Strategy B	3754.40	7012.84	1.86
Strategy A	4673.34	8306.89	1.40
Strategy D	4676.62	9154.62	258.45

Table 8: Total number of infections averted and total cost with their ICER.

Strategies	Total infections averted	Total cost ($)	ICER
Strategy A	4673.34	8306.89	1.78
Strategy D	4676.62	9154.62	258.45

Pontryagin is used to obtain the necessary condition of the optimal control problem. The cost-effectiveness of each control combination is then investigated. As a result, based on the optimality system simulation results and cost-effectiveness analysis, we proposed that the combination of treated bed nets, and treatment is the most optimal and least expensive strategy to reduce malaria transmission.

Data Availability

All data were included in the manuscript.

Conflicts of Interest

The authors have no particular conflicts of interest on the manuscript.

References

[1] A. Abdelrazec and A. B. Gumel, "Mathematical assessment of the role of temperature and rainfall on mosquito population dynamics," *Journal of Mathematical Biology*, vol. 74, no. 6, pp. 1351–1395, 2017.

[2] WHO, "World malaria day, report of the World Health Organisation," 2021, http://www.who.int/malaria/media/world-malaria-day-2021/en/.

[3] K. P. Paaijmans, S. Blanford, A. S. Bell, J. I. Blanford, A. F. Read, and M. B. Thomas, "Influence of climate on malaria transmission depends on daily temperature variation," *Proceedings of the National Academy of Sciences*, vol. 107, no. 34, pp. 15135–15139, 2010.

[4] K. O. Okosun, O. Rachid, and N. Marcus, "Optimal control strategies and cost-effectiveness analysis of a malaria model," *Biosystems*, vol. 111, no. 2, pp. 83–101, 2013.

[5] R. Ross, *The Prevention of Malaria*, John Murray, London, 1911.

[6] G. Bhuju, G. R. Phaijoo, and D. B. Gurung, "Mathematical study on impact of temperature in malaria disease transmission dynamics," *Advances in Computing Science*, vol. 1, no. 2, 2018.

[7] S. Olaniyi, K. O. Okosun, S. O. Adesanya, and R. S. Lebelo, "Modelling malaria dynamics with partial immunity and protected travellers: optimal control and cost-effectiveness analysis," *Journal of Biological Dynamics*, vol. 14, no. 1, pp. 90–115, 2020.

[8] S. F. Abimbade, S. Olaniyi, and O. A. Ajala, "Recurrent malaria dynamics: insight from mathematical modelling," *The European Physical Journal Plus*, vol. 137, no. 3, pp. 1–16, 2022.

[9] T. D. Keno, O. D. Makinde, and L. L. Obsu, "Modelling and optimal control analysis of malaria epidemic in the presence of temperature variability," *Asian-Europian Journal of Mathematics*, vol. 15, no. 1, 2022.

[10] A. Nwankwo and D. Okuonghae, "Mathematical assessment of the impact of different microclimate conditions on malaria transmission dynamics," *Mathematical Biosciences*, vol. 16, no. 3, pp. 1414–1444, 2019.

[11] T. D. Keno, O. D. Makinde, and L. L. Obsu, "Impact of temperature variability on SIRS malaria model," *Journal of Biological Systems*, vol. 29, no. 3, pp. 773–798, 2021.

[12] F. B. Agusto, N. Marcus, and K. O. Okosun, "Application of optimal control to the epidemiology of malaria," *Electronic Journal of Differential Equations*, vol. 81, pp. 1–22, 2012.

[13] K. O. Okosun, O. Rachid, and N. Marcus, "Optimal control analysis of a malaria disease transmission model that includes treatment and vaccination with waning immunity," *Biosystems*, vol. 106, no. 2-3, pp. 136–145, 2011.

[14] R. Leiton, P. Jhoana, M. Aguilar, and E. Ibarg, "An optimal control problem applied to malaria disease in Colombia," *Applied Mathematical Sciences*, vol. 12, no. 6, pp. 279–292, 2018.

[15] S. Olaniyi, K. O. Okosun, S. O. Adesanya, and E. A. Areo, "Global stability and optimal control analysis of malaria dynamics in the presence of human travelers," *Open Forum Infectious Diseases*, vol. 10, no. 1, pp. 166–186, 2018.

[16] T. D. Keno, O. D. Makinde, and L. L. Obsu, "Optimal control and cost effectiveness analysis of SIRS malaria disease model with temperature variability factor," *Journal of Mathematical and Fundamental Sciences*, vol. 53, no. 1, pp. 134–163, 2021.

[17] M. Ghosh, S. Olaniyi, and O. S. Obabiyi, "Mathematical analysis of reinfection and relapse in malaria dynamics," *Applied Mathematics and Computation*, vol. 373, article 125044, 2020.

[18] P. Van den Driessche and J. Watmough, "Reproduction numbers and sub-threshold endemic equilibria for compartmental models of disease transmission," *Mathematical Biosciences*, vol. 180, no. 1-2, pp. 29–48, 2002.

[19] O. S. Obabiyi and S. Olaniyi, "Global stability analysis of malaria transmission dynamics with vigilant compartment," *Electronic Journal of Differential Equations*, vol. 2019, no. 9, pp. 1–10, 2019.

[20] M. Osman and I. Adu, "Simple mathematical model for malaria transmission," *Journal of Advances in Mathematics and Computer Science*, vol. 25, no. 6, pp. 1–24, 2017.

[21] L. B. Dano, K. P. Rao, and T. D. Keno, "Fractional order differential equations for chronic liver cirrhosis with frequent hospitalization," *BMC Research Notes*, vol. 15, no. 1, pp. 1–10, 2022.

[22] J. P. LaSalle, "The stability of dynamical systems, society for industrial and applied mathematics," *Proceedings of the Conference Series in Applied Mathematics*, vol. 25, 1976.

[23] O. D. Makinde and K. O. Okosun, "Impact of chemo-therapy on optimal control of malaria disease with infected immigrants," *Biosystems*, vol. 104, no. 1, pp. 32–41, 2011.

[24] N. Chitnis, J. M. Hyman, and J. M. Cushing, "Determining important parameters in the spread of malaria through the

sensitivity analysis of a mathematical model," *Bulletin of Mathematical Biology*, vol. 70, no. 5, pp. 1272–1296, 2008.

[25] L. B. Dano, K. P. Rao, and T. D. Keno, "Modeling the combined effect of hepatitis B infection and heavy alcohol consumption on the progression dynamics of liver cirrhosis," *Journal of Mathematics*, vol. 2022, no. 19, Article ID 6936396, 18 pages, 2022.

[26] T. D. Keno, L. B. Dano, and G. A. Ganati, "Optimal control and cost-effectiveness strategies of malaria transmission with impact of climate variability," *Journal of Mathematics*, vol. 2022, Article ID 5924549, 20 pages, 2022.

[27] G. J. Abiodun, R. Maharaj, P. Witbooi, and K. O. Okosun, "Modelling the influence of temperature and rainfall on the population dynamics of Anopheles arabiensis," *Malaria Journal*, vol. 15, no. 1, pp. 288–324, 2016.

[28] L. S. Pontryagin, V. G. Boltyanskii, R. V. Gamkrelidze, and E. F. Mishchenko, *The Mathematical Theory of Optimal Processes*, Wiley, New York, 1962.

[29] K. O. Okosun and O. D. Makinde, "A co-infection model of malaria and cholera diseases with optimal control," *Mathematical Biosciences*, vol. 258, pp. 19–32, 2014.

[30] K. O. Okosun and O. D. Makinde, "Optimal control analysis of malaria in the presence of non-linear incidence rate," *Applied and Computational Mathematics*, vol. 12, no. 1, pp. 20–32, 2013.

[31] R. Jan, M. A. Khan, and J. F. Gómez Aguilar, "Asymptomatic carriers in transmission dynamics of dengue with control interventions," *Optimal Control Applications & Methods*, vol. 41, no. 2, pp. 430–447, 2020.

[32] S. Olaniyi, M. Mukamuri, K. O. Okosun, and O. A. Adepoju, "Mathematical analysis of a social hierarchy-structured model for malaria transmission dynamics," *Results in Physics*, vol. 34, article 104991, 2022.

[33] C. T. Deressa and G. F. Duressa, "Modeling and optimal control analysis of transmission dynamics of COVID-19: the case of Ethiopia," *Alexandria Engineering Journal*, vol. 60, no. 1, pp. 719–732, 2021.

[34] L. L. Obsu and S. F. Balcha, "Optimal control strategies for the transmission risk of COVID-19," *Journal of Biological Dynamics*, vol. 14, no. 1, pp. 590–607, 2020.

[35] W. H. Fleming and R. W. Rishel, *Deterministic and stochastic optimal control*, Springer, New York, USA, 1975.

[36] S. Lenhart and J. T. Workman, *Optimal Control Applied to Biological Models*, CRC Mathematical and Computational Biology Series, 2007.

[37] G. T. Tilahun, O. D. Makinde, and D. Malonza, "Modelling and optimal control of typhoid fever disease with cost-effective strategies," *Journal of Theoretical Medicine*, vol. 2017, article 2324518, 16 pages, 2017.

[38] H. W. Berhe, O. D. Makinde, and D. Malonza, "Co-dynamics of measles and dysentery diarrhea diseases with optimal control and cost-effectiveness analysis," *Applied Mathematics and Computation*, vol. 347, pp. 903–921, 2019.